GEOPHYSICS, VOL. 63, NO. 4 (JULY-AUGUST 1998); P. 1348–1356, 6 FIGS., 3 TABLES.

Large near-surface velocity gradients on shallow seismic reflection data

Richard D. Miller* and Jianghai Xia*

ABSTRACT

Extreme velocity gradients occasionally present within near-surface materials can inhibit optimal common midpoint (CMP) stacking of near-surface reflection arrivals. For example, abrupt increases in velocity are observed routinely at the bedrock surface and at the boundary between the vadose and the saturated zone. When a rapid increase in near-surface velocity is found, NMO correction artifacts manifested on CMP gathers as sample reversion, sample compression, or duplication of reflection wavelets can reduce S/N ratio on stacked data or can stack coherently. Elimination of these nonstretch-related artifacts using conventional NMO-stretch muting requires near-vertically incident reflection arrivals and allowable stretch ratios as small as 5% in some shallow environments. Radical allowable stretch mutes are not a feasible means to subdue these artifacts if high-amplitude coherent noise on near-offset traces inhibits identification and digital enhancement of shallow reflections. On most shallow seismic reflection data, long-offset reflection arrivals (but less than wide angle) are critical to the generation of an interpretable stacked section. The difference in offset between the optimum window for shallow reflections within unsaturated sediments and reflections from the underlying saturated or consolidated-material portion of the section inherently limits the effectiveness of conventional NMO corrections. Near-surface average velocity increases of 200% in less than two wavelengths and at two-way traveltimes less than 60 ms are not uncommon on shallow reflection data. Near-surface reflections separated by large velocity gradients can rarely be accurately or optimally CMP processed using conventional approaches to NMO corrections. Large velocity-gradient shallow reflection data require segregation of shallow lower velocity reflections from higher velocity reflections during processing to maximize the accuracy and resolution potential of the stacked section, as shown by examples herein.

INTRODUCTION

Contrasts and comparisons between conventional seismic reflection (predominantly used for petroleum exploration) and shallow seismic reflection (which focuses on environmental, engineering, mining, and groundwater problems) consistently suggests reciprocity of methodologies and techniques is not automatic and is more than a simple relationship of scale (Steeples and Miller, 1990; Miller, 1992; Steeples et al., 1995). This lack of linearity is not surprising when considering the diverse propagation characteristics of source-generated noise in the early time portion of a seismogram. Shallow seismic reflection studies routinely have been plagued by overwhelming near-source noise arriving within the optimum time and offset window for most shallow reflecting events.

One of the more troublesome and potentially detrimental near-surface problems relates to the occasional extreme contrast in interval velocity between the unconsolidated portion of the vadose zone and the bedrock surface or water table (Birkelo et al., 1987; Miller and Xia, 1997). Degradation in frequency content of shallow reflection wavelets during the transformation from shot gathers to common midpoint (CMP) stacked sections has been correlated to insufficient compensation for statics, incomplete correction for nonvertical incidence, changes in reflection wavelet with source-to-geophone offset, and source or receiver variability (Pullan et al., 1991).

Adjusting reflection wavelets on seismic data to compensate for nonvertically incident raypaths is necessary prior to CMP stacking (Mayne, 1962). Because average velocity normally increases with depth, the normal moveout (NMO) curves for a series of reflection events will possess decreasing curvature with increasing depth for a given offset window (Yilmaz, 1987). Correcting or flattening these curves to allow enhancement stacking of all reflection wavelets from a particular reflector,

Manuscript received by the Editor April 25, 1997; revised manuscript received November 25, 1997.
*Kansas Geological Survey, 1930 Constant Avenue, Lawrence, Kansas 66047. E-mail: rmiller@kgs.ukans.edu; jxia@kgs.ukans.edu.

regardless of source-to-receiver offset, requires a dynamic adjustment to each sample. When a time-variable velocity function is defined, this dynamic adjustment is accomplished by stretching the time separation between individual samples in a fashion consistent with the velocity, depth, and source-to-receiver offset of a particular wavelet. The velocity value used to adjust data to flatten a hyperbola is referred to as *NMO velocity*.

If not accompanied by a very aggressive mute (Miller, 1992), artifacts produced by the stretching process (Buchholtz, 1972; Dunkin and Levin, 1973) can decrease resolution potential, alter amplitude characteristics, and reduce the S/N ratio on shallow reflection data. Sample compression, sample reversion, and duplication of the reflection wavelet are nonstretch-related artifacts associated with NMO corrections that can be prevalent when an initially low average velocity increases several hundred percent within a relatively short depth range. It is rare to see these nonstretch artifacts on conventional data sets with their greater depths of interest and more stable average velocities. Adjustments for NMO on shallow reflection data generally are complicated by the high frequency of the data, low S/N ratio, high static-shift-to-dominant-period ratio, and a minimal number of traces with identifiable reflections at near-source offsets and within the optimum reflection window.

Abrupt velocity increases from subsonic to more than six times the speed of sound in air within vertical distances less than 20 m have been measured on shallow seismic reflection data (Birkelo et al., 1987; Miller et al., 1989; Goforth and Hayward, 1992). Velocity disparities of this magnitude generally are encountered between unconsolidated and consolidated sediments as well as between the saturated and unsaturated zones. Increases in compressional wave velocities of 100% to 800% have been observed on shallow reflection data when several meters of dry, unconsolidated materials overlie a consolidated bedrock (Miller et al., 1989; Goforth and Hayward, 1992). These geologic settings can produce both bedrock reflections (from <20 m) with NMO velocities of around 400 m/s and reflections from layers only tens of meters deeper than bedrock with NMO velocities in excess of 1500 m/s (Figure 1a). This almost four-times increase in average velocity can occur in less than 30 ms two-way traveltime. Bedrock-reflection hyperbolas commonly observed when overlying sediments are slow, dry, and unconsolidated tend to interfere with and cross higher velocity reflection hyperbolas from within the consolidated section.

A large velocity gradient is also likely present near the water table in unconsolidated material (Birkelo et al., 1987; Miller and Xia, 1997). The dramatic increase in velocity across the water table can be attributed directly to saturation (Elliott and Wiley, 1975). Reasonable variations in unconsolidated lithology, such as increasing the clay content by 30%, can only change compressional wave velocities by 30% to 40% (Marion et al., 1992). NMO velocities within unconsolidated materials at or above the water table can be less than 250 m/s, while NMO velocities immediately below the water table may exceed 1250 m/s (Figure 1b). This five-times increase in NMO velocity could easily occur in less than 20 ms two-way timetravel. Reflection hyperbolae from reflectors at or above the water table surface can possess sufficient curvature to prevent coincident NMO correction of reflections from both above and below the water table surface.

Near-vertically incident reflections are necessary to generate a representative stacked section when shallower reflections intersect deeper reflections at offsets less than the optimum reflection window. Near-vertically incident reflections by nature are recorded within the noise cone that follows the direct wave, air-coupled wave, ground roll, and refractions. The practical recording of reflections after the initial arrival of ground roll and air-coupled wave has severely limited shallow reflection techniques (Slaine et al., 1990). Confident separation from noise (ground roll and the air-coupled wave) and enhancement of reflection events within the noise cone requires multichannel recording. Enhancing reflections within the noise cone when the S/N ratio is low has been successful in a few

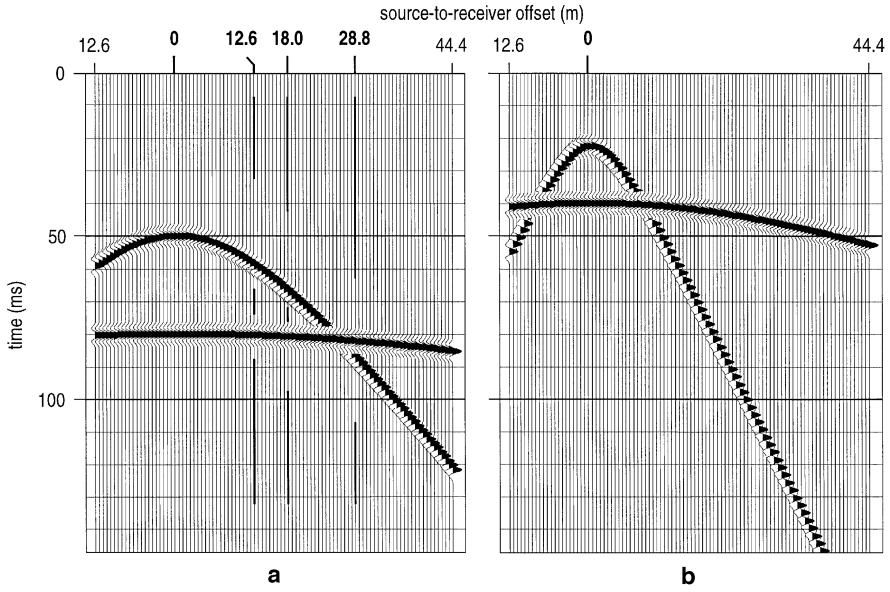

FIG. 1. Reflection models possessing 200-Hz wavelets with large velocity gradients: (a) 400-m/s unconsolidated material over a 10-m-deep high-velocity bedrock material with a 1500-m/s reflection 50 m deeper; (b) 250-m/s reflection from a 2.8-m-deep water table and 1250-m/s reflection from a 27-m-deep intraalluvial layer.

cases (Miller et al., 1995a,b; Merey et al., 1992) but is generally difficult.

Stacking velocities traditionally have been defined for 2-D reflection surveys using constant-velocity stacks, curve fitting to CMP or shot gathers, or semblance routines (Yilmaz, 1987). These techniques are quite effective and well suited for approximating the stacking velocity of each reflection event individually. However, using multiple iterations of constant-velocity analysis to define the best time-variable velocity function for a series of shallow reflection events assumes a gradually increasing average velocity within the earth's near surface. Defining a rapid change in stacking velocity within a relatively short time window will compromise the precision of an individual stacked near-surface reflection when compared to that same reflection stacked using a constant NMO velocity. Using constant-velocity analysis techniques to appraise the detrimental effects of large velocity-gradient NMO corrections is restricted by its very nature. Constant-velocity analysis techniques alone will neither expose high-velocity gradient artifacts nor allow evaluation of the effectiveness of radical stretch mutes to eliminate these artifacts.

MODEL STUDIES

To comprehend fully the root and breadth of the large velocity-gradient problem on shallow seismic reflection data, it is helpful to observe NMO correction artifacts on model data. The models (Figure 1) used to demonstrate these NMO correction artifacts replicate two different but real near-surface geologic settings (Birkelo et al., 1987; Goforth and Hayward, 1992). Trace spacing of these models is 0.6 m, and the source is located at trace 22. The model data display only reflection hyperbolas as defined by the traveltime equation. Because the traveltime equation is the basis for the NMO correction, these models are sufficient to simulate reality.

Starting from the traveltime equation,

$$t^2 = t_0^2 + \frac{x^2}{v^2}, \tag{1}$$

where t is two-way traveltime, x is the distance (offset) between the source and receiver position, v is the NMO velocity of the medium above the reflecting interface, and t_0 is two-way zero-offset reflection traveltime, the arrival time of a reflection wavelet (t) can be determined for any given offset (x). For the case of the models used here (Figure 1), the reflection hyperbolae can be defined by traveltime pairs, $(t_0)_1$, t_1 and $(t_0)_2$, t_2. The value of these traveltime pairs is governed by

$$t_1^2 = (t_0)_1^2 + \frac{x^2}{v_1^2},$$

and (2)

$$t_2^2 = (t_0)_2^2 + \frac{x^2}{v_2^2},$$

where $(t_0)_1$ and $(t_0)_2$ are the zero offset times for the reflection events, v_1 and v_2 are the NMO velocity of $(t_0)_1$ and $(t_0)_2$, and t_1 and t_2 are the traveltimes for the same reflection events at offset x. Nonstretch artifacts will not occur after conventional NMO corrections as long as the average earth velocities increase gradually with depth such that the relationship $(t_0)_2 > (t_0)_1$ and $t_2 > t_1$ is true throughout in the optimum range of x. These time relationships are influenced strongly by the shallowest reflection NMO velocity and the rate of change in NMO velocities of consecutively deeper reflections.

The rate of change in velocity between two zero-offset reflection times $(t_0)_1$ and $(t_0)_2$ must not increase; otherwise, v_2 violates the relationship

$$v_2 \le \sqrt{\frac{x^2}{\frac{x^2}{v_1^2} + (t_0)_1^2 - (t_0)_2^2}}. \tag{3}$$

When the maximum rate of change in velocity is such that v_2 disregards inequality (3), a phenomenon we call *reversion* occurs. Reversion is the reversal of adjacent groups of samples from their original recording order as a result of the NMO correction. NMO-corrected wavelets originally recorded within a time and offset window where reversion conditions exist appear coherent, much higher frequency, spatially mismapped, and with dramatically different phase. Reversion as described here is not a stretch artifact; however, many times in practice it is unknowingly suppressed by the application of a severe allowable stretch mute.

Reversion in some cases is accompanied by sample compression. Using the previously defined model (Figure 1a), the NMO velocity increases from 400 m/s at $(t_0)_1 = 50$ ms to 1500 m/s at $(t_0)_2 = 80$ ms, which results in a velocity gradient of 36.7 m/s/ms. This velocity gradient violates inequality (3), setting up a reversion and compression environment at certain offsets. Each sample of the 28.8-m source-to-receiver offset trace can be mapped from its original recording time to one or more vertically incident arrival times (Table 1). Compression is evident, for example, between 71 and 88 ms where 17 ms will be squeezed into the 8 ms between 50 and 58 ms (Table 1). Accompanying this

Table 1. Time shifts by NMO correction and their stretching percent (offset = 28.8 m). Data in this table are associated with Figure 2a and were calculated using equation (1).

t_0 (ms)	v (m/s)	Before NMO correction (ms) (Figure 1a)	After NMO correction (ms) (Figure 2a)	Δt (ms)	$\Delta t/t_0$ (%)
40	400	**82**	40	42	105
42	400	83	42	41	98
44	400	84	44	40	91
46	400	85	46	39	85
48	400	87	48	39	81
50	400	88	50	38	76
52	473	**80**	52	28	54
54	546	75	54	21	39
56	620	73	56	17	30
58	693	71	58	13	22
60	766	71	60	11	18
62	839	71	62	9	15
64	912	71	64	7	11
66	986	72	66	6	9
68	1059	73	68	5	7
70	1132	74	70	4	6
72	1205	76	72	4	6
74	1278	77	74	3	4
76	1352	79	76	3	4
78	1426	81	78	3	4
80	1500	**82**	80	2	3
82	1500	84	82	2	2
84	1500	86	84	2	2

sample compression is reversion, which maps the data sample at 71 ms to 58 ms, while the 88-ms sample goes to 50 ms. A wavelet originally recorded within the 71 to 88 ms time window (Figure 1a) will be compressed in time from 17 to 8 ms and reversed from its original recording order by the NMO correction (Figure 2a). This compression and reversion appears as high-frequency waveforms (W2-2) on the NMO gather (Figure 2a). Elimination of this artifact using a stretch mute would require a 22% limit on the maximum allowable stretch (Table 1). When inequality (3) is violated, sample reversion may be accompanied by sample compression.

The bedrock reflection model (Figures 1a and 2a) also possesses a reversion environment not evident on the model gather for samples recorded on the 18-m trace (Table 2). Reversion would be observed if waveforms were present between 63 and 67 ms. The sample at 67 ms before NMO-correction is moved to a time of 50 ms on the NMO-corrected data while the sample at 63 ms is moved to 54 ms. A minimum allowable stretch mute of 17% is required to suppress this incidence of reversion without compression.

Another phenomenon associated with the NMO correction of large near-surface velocity gradient data is *multiple wavelet mapping*. The NMO mapping of a reflection wavelet into more than one location is only a problem when the velocity gradient is large. A fully developed suite of artifacts is evident on unmuted NMO-corrected model data (Figure 2). The crossover of two reflection arrivals occurs when offset equals 25.8 m. In the near-offset range (offset < 25.8 m), there are two wavelet locations (W1-1 and W1-2) mapped by the NMO equation for each of the reflection wavelets. The shallowest reflection event occupies time samples around 67 ms on the 18.0-m offset trace (Table 2). After NMO correction, the sample at 67 ms is mapped both to 50 ms (W1-1) and 64 ms (W1-2) (Figure 2a). For this example, an allowable stretch of less than 5% is necessary to remove all the nonstretch artifact, which also removes the correctly mapped wavelet at 50 ms, which was stretched 34%. Multiple-wavelet mapping can be effectively suppressed and in some cases removed with severe stretch mutes.

The multiple-wavelet mapping phenomenon also tends to smear waveforms. Waveform smearing, however similar in appearance to sample stretch, is not related to stretch. Smearing can be observed between 50 and 58 ms on near-offset traces (8.4–13.8 m) of the NMO corrected model data (Figure 2a). The stretching percent (Table 3) demonstrates that this smear in the waveform evident between 50 to 58 ms is not stretch and will not be muted completely even with a stretching limit as low as 10%. A stretching limit of less than 5% is required to completely eliminate the smear artifact on these NMO-corrected model data. Only traces at very near offset will survive the 5% mute necessary to suppress this smear.

Table 2. Time shifts by NMO correction and their stretching percent (offset = 18.0 m). Data in this table are associated with Figure 2a and were calculated using equation (1).

t_0 (ms)	v (m/s)	Before NMO correction (ms) (Figure 1a)	After NMO correction (ms) (Figure 2a)	Δt (ms)	$\Delta t/t_0$ (%)
47	400	65	47	18	38
48	400	66	48	18	38
49	400	67	49	18	37
50	400	**67**	50	17	34
51	437	66	51	15	29
52	473	64	52	12	23
53	510	64	53	11	21
54	546	63	54	9	17
55	583	63	55	8	15
56	620	63	56	7	13
57	655	63	57	6	11
58	693	64	58	6	10
59	728	64	59	5	8
60	766	65	60	5	8
61	801	65	61	4	6
62	839	66	62	4	6
63	874	66	63	3	5
64	912	**67**	64	3	5
65	948	68	65	3	5
66	986	68	66	2	3
67	1023	69	67	2	3

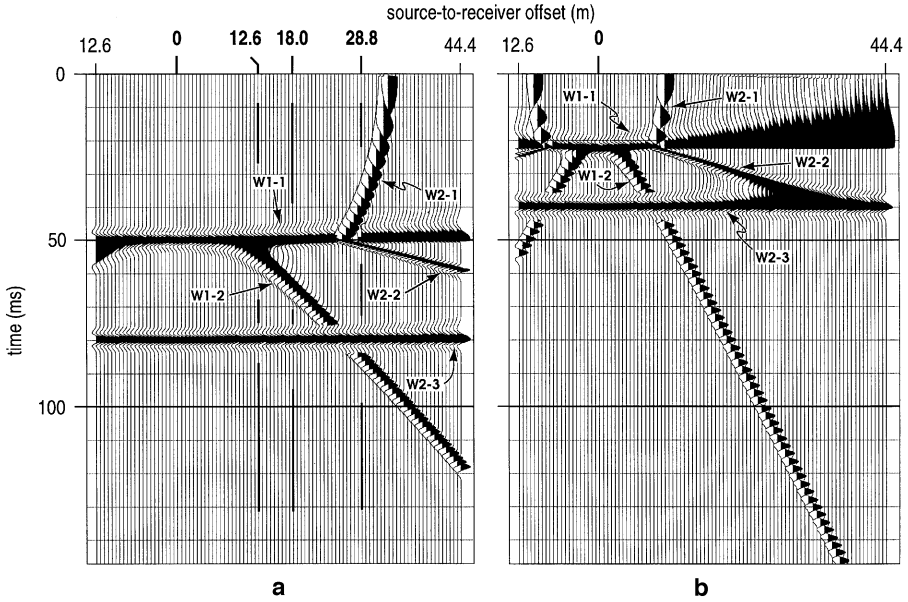

FIG. 2. Moved-out gathers (Figure 1) at model velocities. (a) Effects such as stretch, sample reversion, sample compression, wavelet smear, and duplicate wavelet mapping are identifiable. (b) At 0.6 m trace spacing, only 2 to 3 near-vertical traces provide a minimally distorted water table reflection.

In the far-offset range (offset > 25.8 m), three waveforms (W2-1, W2-2, and W2-3) are mapped by the NMO equation from a single reflection wavelet (Figure 2a). On the 28.8-m offset trace (Table 1) the deepest reflection wavelet originally recorded at 82 ms (Figure 1a) is represented three times on the NMO section (Figure 2a). The three waveforms can be observed at around 40 ms (multiple wavelet mapping), 52 ms (reversed and compressed), and 80 ms (correct location). Suppressing the two waveforms that are artifacts (40 ms and 52 ms) would require a 50% maximum allowable stretch limit.

DATA EXAMPLE

NMO artifacts would not require attention if near-vertically incident reflected energy could routinely be acquired and enhanced on shallow seismic reflection data. However, rarely on shallow reflection data are near-offsets alone sufficient to generate the highest quality and most representative CMP stacked section. Producing the optimum CMP stacked section when the reflections of interest are above and below or within a rapidly changing velocity environment requires a thorough understanding of the types of energy recorded and where each type is prominent on both shot and CMP gathers.

Table 3. Time shifts by NMO correction and their stretching percent (offset = 12.6 m). Data in this table are associated with Figure 2a and were calculated using equation (1).

t_0 (ms)	v (m/s)	Before NMO correction (ms) (Figure 1a)	After NMO correction (ms) (Figure 2a)	Δt (ms)	$\Delta t/t_0$ (%)
48	400	57	48	9	19
49	400	58	49	9	18
50	400	59	50	9	18
51	437	59	51	8	16
52	473	58	52	6	12
53	510	58	53	5	9
54	546	59	54	5	9
55	583	59	55	4	7
56	620	60	56	4	7
57	655	60	57	3	5
58	693	61	58	3	5
59	728	61	59	2	3
60	766	62	60	2	3

A shallow seismic reflection survey acquired in eastern Minnesota, USA, designed to image targets from about 5 to 50 m experienced the large velocity gradient problem. In general glacial/alluvial geologic settings such as the one in which these data were acquired are relatively common in the north-central United States and into Canada. From velocity analysis and borehole measurements the velocity increases from just under 350 m/s to over 1500 m/s at about 6 m, a depth consistent with the water table surface. A spectral-balanced shot gather from this data set demonstrates the dramatic change in curvature of reflections from at or just below the water table to below the bedrock surface (Figure 3a). Interpreting reflections after the arrival of groundroll, direct wave, or air-coupled waves, as well as the shallow low-velocity reflection at around 40 ms, is nearly impossible. It is critical to incorporate extremely close offsets on data such as these to optimize the accuracy and quality of the shallowest as well as deeper reflections on a final stacked section.

Model reflection arrivals that substantially replicate the reflection arrivals of these real data can be used to observe large velocity gradient artifacts of the NMO process (Figure 3b). Without a doubt, the preferred reflection arrivals for incorporation into a CMP stacked section arrive at zero or near-zero offsets and prior to the crossover of deeper reflections by shallower reflections. This is in part because near-vertical arrivals are subject to only minimal NMO correction artifacts. Unfortunately, the best velocity control requires inclusion of reflected energy from source offsets and times susceptible to reversion,

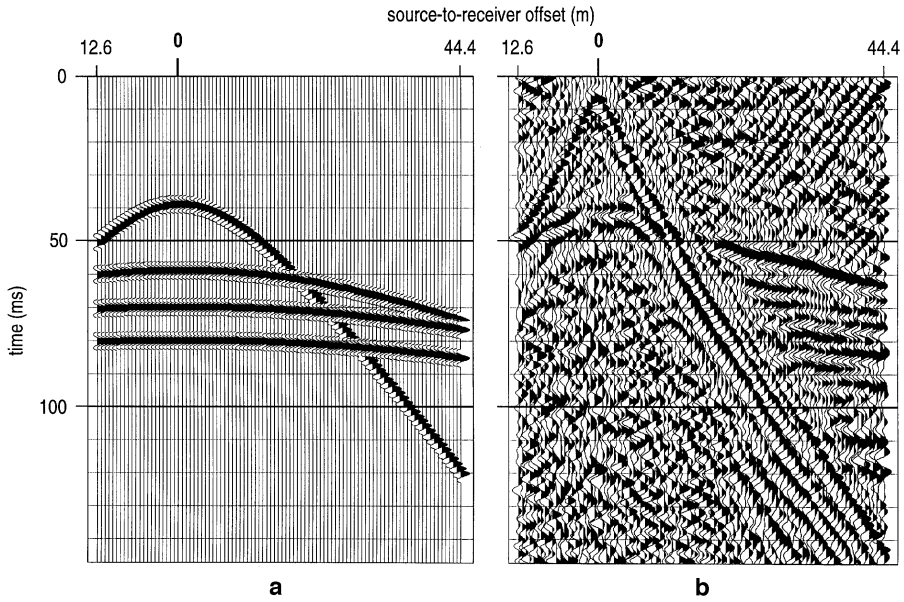

FIG. 3. Representative shot gather from glacial/alluvial setting in eastern Minnesota. (a) Model of four reflection events consistent with real data. (b) Digitally filtered and scaled shot gather showing the offset-dependent nature of the shallow reflections.

compression, and multiple wavelet mapping when a large velocity gradient is defined. As demonstrated by these data (Figure 3a), shallower reflections can arrive after the deeper reflections that are necessary to produce a high-quality stacked section. The four reflection arrivals that make up the model are from 7.6 m deep with an NMO velocity of 390 m/s, 30 m deep with an NMO velocity of 990 m/s, 50 m deep with an NMO velocity of 1410 m/s, and 60 m deep with an NMO velocity of 1500 m/s. The 200-Hz, zero-phase reflection wavelets (Figure 3b) simulate the waveforms of the four primary reflecting horizons interpretable on the real data.

Correcting the model gather (Figure 3b) for nonvertical incidence using a conventional approach requires individual sample adjustment as mapped by a time-and-space variable velocity function and a maximum allowed sample stretch. Nonstretch artifacts of the NMO correction process for the four-reflection model (Figure 4a) are consistent with those described for the previous two-reflection model (Figure 2). Besides the correctly mapped reflection arrivals equivalent to W1-1 and W2-3 (of Figure 2), three reversion and compression artifacts equivalent to W2-2 (of Figure 2) and three mismapped artifacts equivalent to W2-1 (of Figure 2) are all evident on the NMO-corrected gather without a stretch mute (Figure 4a). Also noteworthy is how the multiple mapping phenomena has truncated the lower portion of the overstretched shallow-reflection wavelet at long offset. The decrease of apparent frequency through wavelet elongation of correctly mapped reflection arrivals at longer offsets is the only stretch artifact apparent on the NMO-corrected model gather.

NMO stretch muting is technically not designed to eliminate or even subdue nonstretch-related artifacts, but it can be used quite effectively in that capacity. A 50% stretch mute is relatively severe from a conventional perspective but is the maximum allowable stretch mute that can eliminate the smear between reversion and compression artifacts and the correct mapping of the 60-ms reflection on longer offset traces

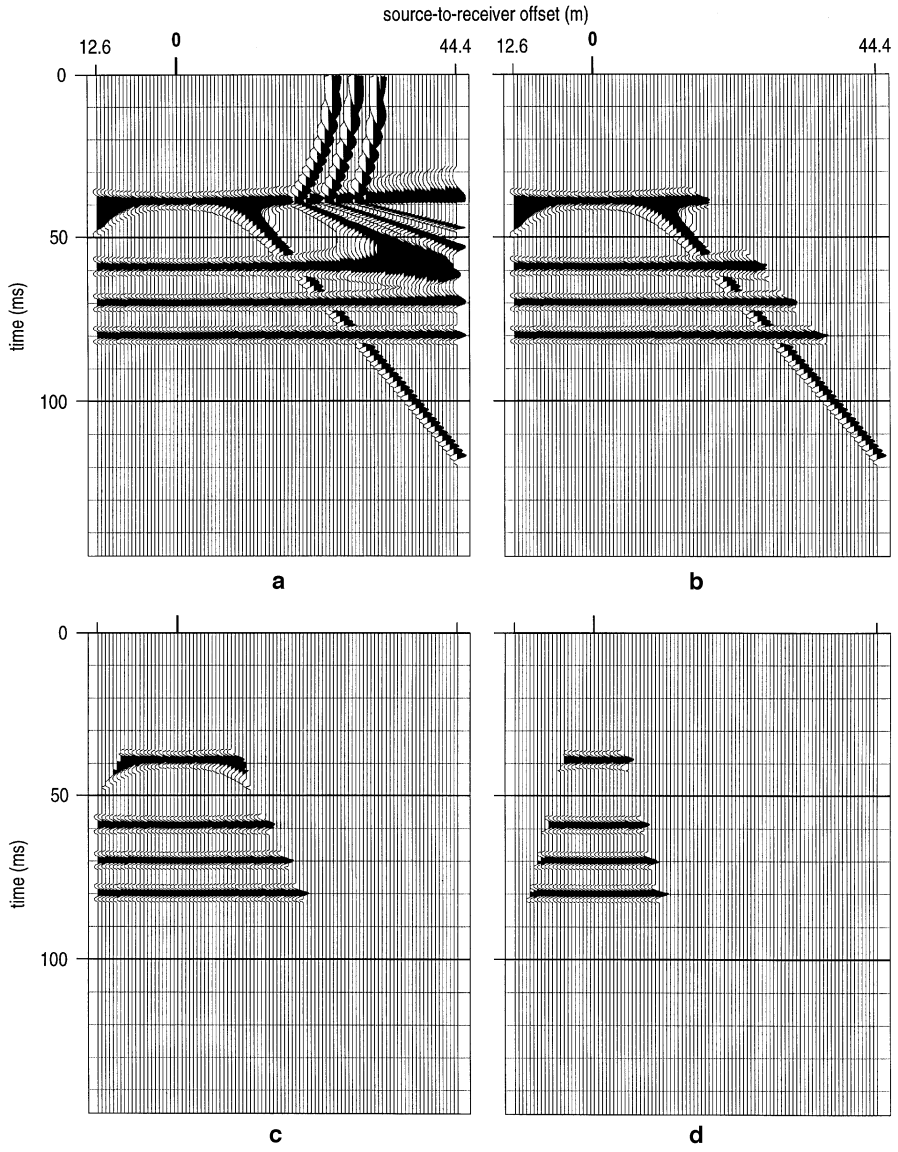

FIG. 4. Moved-out gather using a time-variable velocity function: (a) no stretch mute, (b) 50% stretch mute, (c) 17% stretch mute, and (d) 5% stretch mute.

(Figures 4a and 4b). Complicating the use of a 50% stretch mute is the fact that the highest S/N ratio portion of the higher velocity reflection arrivals will be muted with a 50% maximum allowable stretch mute (Figures 3 and 4). A stretch mute targeting nonstretch NMO correction artifacts in a shallow large velocity gradient setting will eliminate high-quality reflections when the mute is used as technically designed and conventionally done.

A maximum allowable stretch as small as 5% may be necessary to minimize the contribution of the nonstretch NMO correction artifacts of a shallow, low-velocity reflection. A 50% stretch mute eliminates all nonstretch artifacts of the NMO correction except two different manifestations related to the shallowest reflection (Figure 4b). The coherent hyperbolic arrival after NMO correction with a 50% maximum allowable stretch is a multiple wavelet mapping remnant of the shallowest reflection (Figure 4B). Smearing at the intersection of this hyperbolic remnant and the correctly moved-out portion of the wavelet is evident on both the 50% and 17% maximum allowable stretch gathers (Figures 4b and 4c). A 5% maximum allowed stretch mute appears to eliminate all nonstretch artifacts associated with the NMO correction processes (Figure 4d). Reflection arrivals remaining after application of a 5% stretch mute (Figure 4d) are not, however, consistent with the optimum reflection window for the higher velocity reflection arrivals on real data (Figure 3b). This inconsistency inhibits the effectiveness of conventional approaches to NMO correction to suppress all these nonstretch artifacts.

Application of a time-and-space variable-NMO velocity correction and a single maximum allowable stretch mute will not result in the optimum CMP stacked section. A moved-out shot gather after application of a 17% stretch mute demonstrates how inadequately stretch muting alone handles the suppression of artifacts while having a substantially negative effect on the reflection arrivals within the optimum reflection window (Figure 5). No reflection arrivals from the deeper, higher velocity reflectors are evident after the NMO correction. The smear as previously modeled (Figure 4c) at the intersection of the correctly moved-out wavelet and the hyperbolic remnant of the shallow-low-velocity reflection is present near the mute zone at about 40 ms (Figure 5). After NMO correction and a 17% stretch mute, no coherent reflection energy is visible deeper than the 40 ms reflection (Figure 5) while at least four reflection events (Figure 3) are within the optimum reflection window on the filtered and scaled shot gather deeper than the 40-ms reflection.

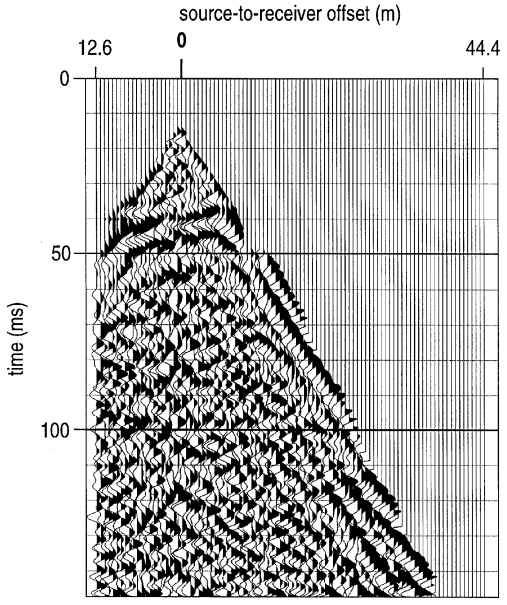

FIG. 5. Filtered and scaled shot gather moved out with a time-variable velocity function appropriate for the reflections between 40 and 120 ms using a 17% stretch mute. This is the same shot gather as in Figure 3b.

ONE SOLUTION: SEGREGATED PROCESSING

Shallow reflection data with a defined large velocity gradient requires special processing to ensure that contributions from all recorded reflected energy are maximized on a CMP stacked section. CMP processing a portion of the entire data set from which the previous real-data example was extracted (Figures 3b and 5) allows evaluation of the effectiveness of segregated processing. The data were split by separating the shallow, low-velocity reflections from deeper, higher velocity reflections to reduce the influence of these nonstretch artifacts (Figure 6). The data were processed identically with the exception of application of the NMO corrections and selected stretch mutes to allow comparisons of segregated versus whole-dataset processing. Processing steps for these data included spectral balancing, muting, geometry designations, NMO correction, and CMP stacking. None of these processes would have resulted in corrections, changes, shifts, or mutes unique to an individual flow.

Segregated processing of the CMP data provided significantly higher S/N ratio and a more accurate stacked section than a single pass of a time-and-space variable NMO velocity correction (Figure 6). The optimum processing flow required separation of the data to allow shallow low-velocity reflections to be NMO corrected separately from deeper higher velocity reflections. Suture zones evident after processing and joining the two parts made surgical muting an inappropriate method of separation. The segregation was accomplished by designations of optimum offset and splitting the data into close and far offsets. The complete time-and-space varying velocity function was applied to the close-offset data with a 5% maximum allowable stretch mute. The far offset traces were NMO corrected without the shallow low velocity defined (because that reflection is not present at longer offsets) and with a 50% maximum allowable stretch mute. The two different offset data sets were then recombined and CMP stacked, producing the highest quality stacked section (Figure 6a). A single-pass time-and-space variable NMO velocity correction with a 50% stretch mute (Figure 6b), a 17% stretch mute (Figure 6c), and a 5% stretch mute (Figure 6d) produced a significantly lower quality stacked section when compared with the segregated application of a time-and-space variable NMO velocity correction using velocity and stretch mutes consistent with the offset-dependent nature of the reflection arrivals.

CONCLUSIONS

With the increase in the number of recording channels available on routine shallow seismic surveys has come the ability to acquire data with offsets conducive to a wider range of reflection depths. The extreme range of optimum reflection windows present when reflectors above and below a large velocity

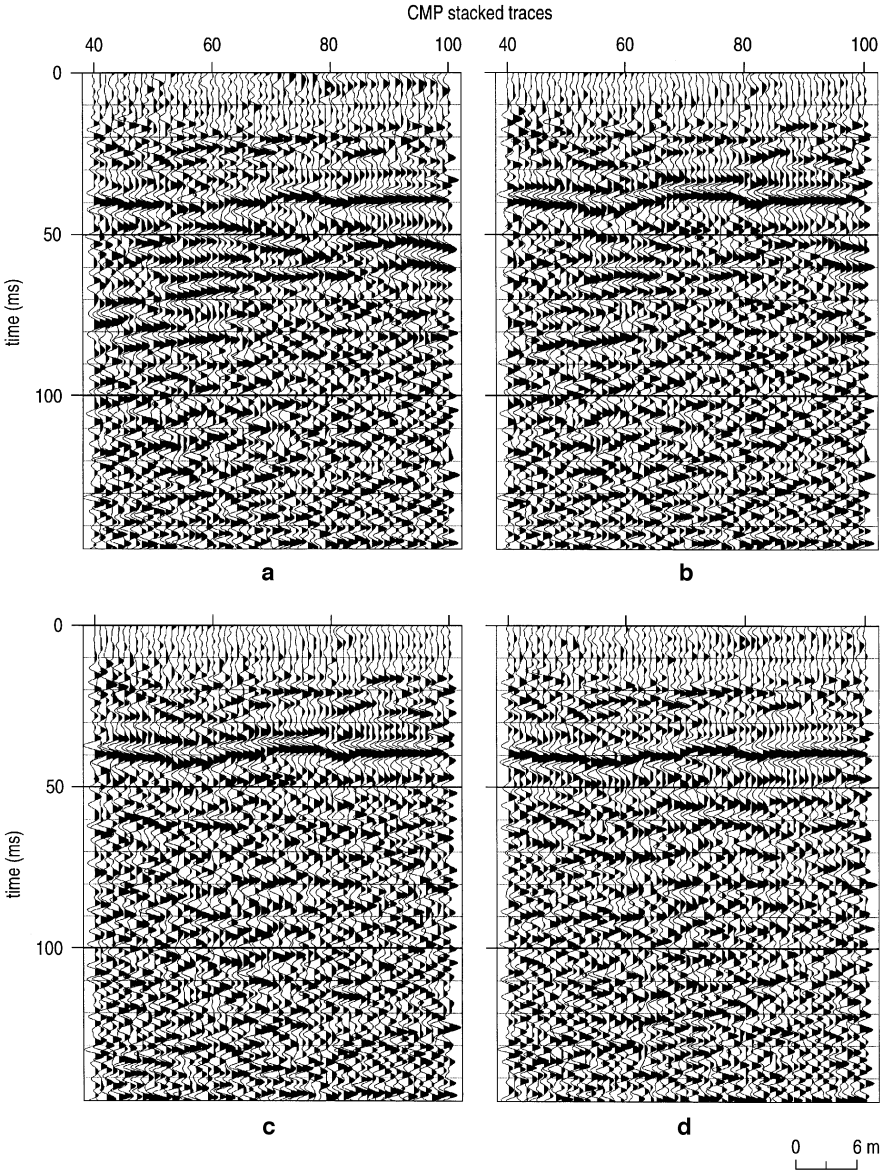

FIG. 6. (a) Optimum processing requires close-offset traces to be NMO corrected with a 5% stretch mute and far-offset traces corrected with NMO velocities below 50 ms and a 50% stretch mute, compared with the complete velocity function, and (b) 50% stretch mute, (c) 17% stretch mute, and (d) 5% stretch mute.

contrast are imaged provides an environment that can violate assumptions of the NMO correction process as routinely applied to conventional data sets. In some settings, due to shallow extreme-velocity contrasts, the velocity gradient may not allow corrections for nonvertical incidence to be performed on reflections above and below this surface within the same processing pass. Artifacts easily undetected during "normal" processing flows and procedures could result in inaccurate and potentially misleading interpretations. One solution to the problem is to use segregated processing in which the long-offset and short-offset data are processed separately and then recombined after NMO is applied.

ACKNOWLEDGMENTS

We thank the US Geological Survey and the US Navy for support of various aspects of this research. We also thank reviewers Don Steeples (Dept. of Geology, University of Kansas) Brad Birkelo (Digital Prospectors, Midland), and Alan Green (ETH Zurich, Switzerland), for their comments. Their input greatly improved this article.

REFERENCES

Birkelo, B. A., Steeples, D. W., Miller, R. D., and Sophocleous, M. A., 1987, Seismic reflection study of a shallow aquifer during a pumping test: Ground Water, **25**, 703–709.

Buchholtz, H., 1972, A note on signal distortion due to dynamic (NMO) corrections: Geophys. Prosp., **20**, 395–402.

Dunkin, J. W., and Levin, F. K., 1973, Effect of normal moveout on a seismic pulse: Geophysics, **38**, 635–642.

Elliott, S. E., and Wiley, B. F., 1975, Compressional velocities of partially saturated, unconsolidated sands: Geophysics, **40**, 949–954.

Goforth, T., and Hayward, C., 1992, Seismic reflection investigations of a bedrock surface buried under alluvium: Geophysics, **57**, 1217–1227.

Marion, D., Nur, A., Yin, H., and Han, D., 1992, Compressional velocity and porosity in sand-clay mixtures: Geophysics, **57**, 554–563.

Mayne, W. H., 1962, Horizontal data stacking techniques: Supplement to Geophysics, **27**, 927–938.
Merey, C., Miller, R. D., Ticken, E. J., and Lewis, J. S., 1992, Hydrogeologic characterization using a shallow seismic reflection survey at Fort Ord, California: 62nd Ann. Internat. Mtg. Soc. Expl. Geophys., Expanded Abstracts, 370–373.
Miller, R. D., 1992, Normal moveout stretch mute on shallow-reflection data: Geophysics, **57**, 1502–1507.
Miller, R. D., Anderson, N. L., Feldman, H. R., and Franseen, E. K. 1995a, Vertical resolution of a seismic survey in stratigraphic sequences less than 100 m deep in southeastern Kansas: Geophysics, **60**, 423–430.
Miller, R. D., Steeples, D. W., and Brannan, M., 1989, Mapping a bedrock surface under dry alluvium with shallow seismic reflections: Geophysics, **54**, 1528–1534.
Miller, R. D., and Xia, J., 1997, High resolution seismic reflection survey to map bedrock and glacial/fluvial layers in Fridley, Minnesota: Symp. on Appl. of Geophys. to Eng. and Environ. Problems, Proceedings, **1**, 281–290.
Miller, R. D., Xia, J., Harding, R. S., Neal, J. T., Fairborn, J. W., and Steeples, D. W., 1995b, Seismic investigation of a surface collapse feature at Weeks Island Salt Dome, Louisiana: AAPG Div. of Environ. Geosci, Jl., **2**, (2), 104–112.
Pullan, S. E., Miller, R. D., Hunter, J. A., and Steeples, D. W., 1991, Shallow seismic-reflection surveys—CDP or "optimum offset"? 61st Ann. Internat. Mtg.: Soc. Expl. Geophys., Expanded Abstracts, 576–579.
Slaine, D., Pehme, P. E., Hunter, J. A., Pullan, S. E., and Greenhouse, J. P., 1990, Mapping overburden stratigraphy at a proposed hazardous waste facility using shallow seismic reflection methods, *in* Ward, S., Ed., Environmental and groundwater, **2**: Soc. Expl. Geophys., 273–280.
Steeples, D. W., Macy, B., Schmeissner, C., and Miller, R. D., 1995, Contrasting near-surface and classical seismology: The Leading Edge, **14**, April, 271–272.
Steeples, D. W., and Miller, R. D., 1990, Seismic reflection methods applied to engineering, environmental, and groundwater problems, *in* Ward, S. Ed., Geotechnical and environmental geophysics, Volume 1: Review and Tutorial: Soc. Expl. Geophys., 1–30.
Yilmaz, O., 1987, Seismic data processing, *in* Doherty, S. M., and Neitzel, E. B., series Eds., Investigations in geophysics, **2**: Soc. Expl. Geophys.